Fibers and Polymers 2022, Vol.23, No.11, 3046-3057
DOI 10.1007/s12221-022-4901-x

ISSN 1229-9197 (print version)
ISSN 1875-0052 (electronic version)

A Study on Structural Characterization of Thermally Stabilized PAN Precursor Fibers Impregnated with Ammonium Bromide before Carbonization Stage

Tuba Demirel[1], Md. Mahbubor Rahman[2,4]*, Kemal Şahin Tunçel[3], and Ismail Karacan[2]*

[1]*Department of Mechanical Engineering, Erciyes University, Kayseri 38039, Turkey*
[2]*Department of Textile Engineering, Erciyes University, Kayseri 38039, Turkey*
[3]*Department of Traditional Crafts, Siirt University, Siirt 56100, Turkey*
[4]*Bangladesh University of Textiles, Tejgaon, Dhaka 1208, Bangladesh*

(Received August 28, 2021; Revised October 19, 2021; Accepted December 5, 2021)

Abstract: Thermal-oxidative stabilization of polyacrylonitrile (PAN) fiber pretreated with ammonium bromide (NH_4Br) was performed in the air atmosphere at temperatures between 200 and 250 °C for periods of 5 to 75 min in a multistep approach. The study demonstrates that the NH_4Br incorporation is highly effective in accelerating nitrile group cyclization by reducing the time required to form a thermally stable structure. After 60 min of the multistep stabilization, NH_4Br incorporated and stabilized PAN was entirely thermally stable, infusible, and non-burning. XRD analysis showed the conversion of the pristine PAN molecular structure from a laterally ordered condition to a very disordered amorphous structure by crosslinking and aromatization process. Infrared analysis indicated rapid and concurrent aromatization and dehydrogenation reactions assisted by the formation of oxygen-containing functional groups. With the progression of the stabilization period, TGA thermograms revealed a comparative increase in thermal stability, as directed by the continuous rise of carbon yield. By decreasing the required time for the stabilization process of PAN fiber, the use of NH_4Br impregnation is expected to enhance carbon fiber productivity at a reduced cost considerably.

Keywords: Polyacrylonitrile, Ammonium bromide, Thermal-oxidative stabilization, Aromatization, Dehydrogenation

Introduction

Carbon fibers have increasingly gained attention in recent times as a potential and promising material in high-performance engineering applications due to their lightweight with excellent mechanical properties [1,2]. Carbon fibers are widely used in the composite form in various fields, including aerospace, automobiles, turbine blade production, pressure vessels, defense, sports, and medical [3,4]. The efficiency of carbon fiber-based composites is strongly dependent on the precursor, which needs to have a high molecular weight [5,6], carbon content [7], and degree of molecular orientation [5,8,9]. PAN-based carbon fibers seem to meet all of these criteria. Polyacrylonitrile fiber is one of the most significant carbon fiber precursors, accounting for nearly 90 % of the global high-performance carbon fiber production [10-12]. PAN-based activated carbon fiber has received increased interest in present times for water treatment and gas adsorption processes, besides its recognized applicability as an outstanding reinforcer for composite materials [4,13].

Thermal-oxidative stabilization (TOS) at 200-300 °C is a crucial step in the production of PAN-based carbon fibers, comprising oxidation, dehydrogenation, cyclization, and tautomerization reactions [14,15]. The TOS process alters the PAN molecular structure from a linear to an intermediate cyclic structure. The modified PAN structure plays a vital role in the subsequent thermal processing stages, including carbonization, graphitization, etc. [16-19]. The oxidation process of thermal stabilization, in which oxygen is added to the PAN molecules and hydrogen is released in the form of H_2O, may influence dehydrogenation mechanisms [19-21]. The chemical composition of the original PAN precursor and stabilization parameters, including heating rate, highest stabilization temperature, stabilization time, and applied environment, are all factors that influence the thermal stabilization reactions. Different reactions take place in different stabilization environments. PAN macromolecules are transformed from a linear to a non-burning ladder-like configuration, allowing for subsequent carbonization at higher temperatures (1000-1700 °C) in the inert environment [22,23].

The stabilization and carbonization steps in carbon fiber production consume around 69 percent of the total energy expenditure. Only the precursor fiber stabilization stage requires around 48 % of expenditure. As a result, the highest quantity of energy and time is expended to ensure that the stabilization step is completed effectively [24,25]. Chemical pretreatments were reported to speed up the TOS process by decreasing the activation energy of the stabilization reactions [26-29]. The incorporation of ammonium persulfate was mentioned to speed up the thermal stabilization reactions, and the initial structure of the PAN multifilaments was rapidly transformed into a completely disordered amorphous phase comprising pre-graphitic structures [29]. The efficacy of halogen-comprising flame-retardants rises in the sequence F < Cl < Br < I. Because of the interference in the

*Corresponding author: mahbub@butex.edu.bd
*Corresponding author: ismailkaracan@erciyes.edu.tr

combustion mechanism, fluorine and iodine-containing flame retardants are not practically utilized. In the gas phase, fluorine cannot perform like a radical interceptor due to the tight bond with carbon. Iodine, on the other hand, is so weakly bonded with carbon that it might well be released by even a small amount of energy applied [30]. Bromide is highly efficacious because of its weak bonding with carbon, allowing it to intervene in a more beneficial way in the combustion phase. Furthermore, it is thought that the HBr as a potent element is released over a confined temperature span, allowing for a greater concentration in the combustion stage. At the combustion phase, there exists a variety of radicals in the vapor state. Generally, the most potent radicals that can assist combustion are $^{\bullet}H$, $^{\bullet}OH$, and others; hence their elimination can aid to inhibit the flame. This would be desirable if these active radicals could be transformed into less reactive radicals in order to attain the target. It is worth noting that in neutralizing active free radicals, all the halogens are efficient [31,32].

The effect of ferric chloride ($FeCl_3$) incorporation was mentioned to stimulate the TOS process by accelerating the incidence of oxidation, cyclization, and dehydrogenation reactions [33]. After impregnation with Cu(I)Cl aqueous solution and thermal stabilization, the tensile properties loss of PAN fibers was reported to be optimized [34]. Ammonium bromide was mentioned in a patent by Sweeny [35] to impregnate with acrylonitrile fiber prior to the thermal oxidation process. However, there was no comprehensive analysis of the physical, mechanical, structural, and thermal properties of the ammonium bromide incorporated and stabilized PAN fiber. In the present investigation, ammonium bromide was used as a catalyst for the aromatization and cyclization reactions during the thermal stabilization process allowing accelerated heating of the samples under investigation to annealing temperatures without unnecessary weight loss or multifilament fusion. The incorporation of ammonium bromide into the PAN molecular structure seems to have resulted in the availability of dehydrogenation and aromatization reactions. These reactions seem to have resulted in the presence of intermolecular and intramolecular crosslinked structures. The apparent interaction between the structures of PAN and ammonium bromide is represented in Figure 1 [36].

The main objective of this study was to perform a thorough investigation on the impact of ammonium bromide incorporation on the molecular structure of PAN fiber followed by thermal stabilization by employing a combination of thermal analysis (TGA), X-ray diffraction, infrared spectroscopy, and physical testing outcomes to monitor and follow the structural conversions with growing stabilization period.

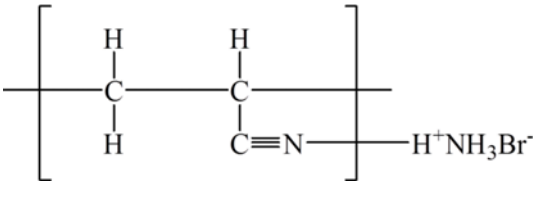

Figure 1. Apparent interaction between the structures of PAN and ammonium bromide.

Experimental

Materials

Commercial textile grade PAN fibers (in non-carbonized/ non-activated form) were collected from AKSA Acrylics Ltd., Yalova, Turkey. The PAN multifilaments utilized in this study had a linear density of 59.68 tex and fiber thickness of 22±0.2 μm. The chemicals including ethanol and ammonium bromide employed in this work were laboratory-grade provided by TEKKIM chemical industries, Turkey.

Samples Preparation

Prior to chemical impregnation, untreated PAN fibers were treated in 10 % aqueous ethanol solution for one hour at room temperature to eliminate impurities from the surface. Afterward, the samples were allowed to dry overnight. Chemical impregnation of the PAN fibers was carried out with the aqueous solution of 5 % NH_4Br at 90 °C temperature for one hour. The pH of the solution was measured as 5.82 at 22.7 °C. NH_4Br incorporated samples were dried at 80 °C for four hours. The impregnated PAN fibers had a linear density value of 61.64 tex, and the chemical integration with fibers was 3.3 %. The NH_4Br impregnated PAN fibers were wrapped on stainless steel rectangular frames to avoid shrinkage and reduction of fiber orientation. The PAN fibers were passed through the multistep TOS process in an air-circulated furnace. The stabilization times of 5, 15, 30, 45, 60, and 75 min were utilized at the temperatures of 200, 210, 220, 230, 240, and 250 °C with a heating rate of 2 °C/min. Afterward, the same heating rate was followed to reach the furnace at room temperature.

Methods

Thermogravimetric (TGA) Analysis

The TGA thermograms of the raw and stabilized specimens were obtained using a Perkin Elmer diamond TGA device. The highest temperature for the TGA measurements was 1000 °C. The temperature was raised at a rate of 10 °C per minute. The temperature adjustment of TGA was accomplished utilizing melting temperature standards of indium, tin, zinc, aluminum, and gold. Weight calibration was performed using 20 mg standard weight at 20 °C in both systems. By means of the TGA results, weight loss (%) and carbon yield (%) values were assessed due to untreated and thermal

stabilized PAN fibers.

Fourier Transform Infrared (FT-IR) Analysis

Infrared spectroscopy is widely used to examine structural changes that occurred during the process of thermal stabilization reactions. A Perkin Elmer® Spectrum 400 infrared spectrometer was employed during the present investigation. For all the samples, 50 interferograms were collected and averaged. Using the curve-fitting techniques and SPECTRUM® software, all the bands were studied where applicable. Finally, all the averaged interferograms were converted by using medium the Norton-Beer apodization function.

X-ray Diffraction (XRD) Analysis

The Bruker® AXS D8 X-ray diffractometer is used for XRD work using current and voltage adjustments of 40 mA 40 kV, respectively. X-ray scattering values were collected for raw and stabilized specimens at 5-35 ° 2θ in reflection mode and were adjusted for Lorentz, polarization, and incoherent scatter aspects.

Burning Behavior Test

The burning (non-flammability) test is a suitable pretesting method to determine textile fiber categories. Stabilized PAN samples were directly exposed to a match flame to determine their burning rate and properties. Afterward, it was removed from the flame and, the burning characteristics were observed. Flameproof test results were classified as pass or fail.

Fiber Thickness Measurement

Fiber thickness measurement was performed using an optical microscope (Nikon ME 600L) for pristine and stabilized PAN fibers. Twenty marks in width were collected from five separate fibers to measure the thickness of the fiber, and the mean value was utilized.

Linear Density Measurement

The linear density values of the samples were evaluated based on the mass (g) per unit length (m). Tex, a typical unit for measuring linear density, is the assessed value of the weight in grams per 1000 meters length of the yarn. By utilizing linear density values, stabilization yield percentage was evaluated, which is the ratio of linear densities of the pristine and the stabilized samples.

Volume Density Measurement

Volume density measurements for the untreated and stabilized samples were acquired utilizing a density gradient device operating at 23±1 °C. To make ready the column for density measurement, isopropyl alcohol (ρ=0.793 g/cm^3) and perchloroethylene (ρ=1.61 g/cm^3) were employed. The gradient column was adjusted by incorporating specific floats of known density.

Mechanical Properties Measurement

PAN fibers were measured by a PROWHITE/Zwick-Roell 1446 tensile machine. The load cell of 25 N with a testing length of 20 mm for stabilized and untreated PAN fibers. In each case, 20 strands were tested, and the average value was calculated.

Data Analysis

IR-Conversion Index Evaluation

The IR-conversion index is commonly utilized to assess the overall quantity of crosslinked ladder structure in the stabilized samples [37] and was calculated using equation (1).

$$\text{IR-Conversion Index (\%)} = \frac{I_0}{I_0 + I_N} \times 100 \quad (1)$$

I_0 indicates the conjugated band intensity at ~1590-1600 cm^{-1}, while I_N indicates the intensity of the nitrile band at ~2242 cm^{-1}.

X-ray Stabilization Index Evaluation

The X-ray stabilization index was calculated employing the peak intensity above that of the baseline, as shown in equation (2) [38].

$$\text{X-ray Stabilization Index (\%)} = \frac{I_0 - I}{I_0} \times 100 \quad (2)$$

I_0 shows the reflectance (100) at 2θ=17 ° of the original PAN fibers, and I indicates the reflectivity (100) at 2θ=17 ° of the oxidized PAN fibers.

Apparent X-ray Crystallinity Evaluation

The apparent X-ray crystallinity (χ_c) is the relationship between the integrated intensity under the resolved peaks and the entire diffusion under the experimental trace [39]. A curve-fitting technique was applied to evaluate exact peak shape characteristics in specified peak heights above baseline to determine X-ray stabilization parameter (%) indices. In the present investigation, the apparent degree of crystallinity was evaluated using equation (3). In this study, the assessment was conducted within a range of 2θ between 5 ° and 35 °.

$$\chi_c = \frac{\int_0^\infty I_{cr}(2\theta)d(2\theta)}{\int_0^\infty I_{tot}(2\theta)d(2\theta)} \quad (3)$$

Apparent Lateral Crystallite Size Evaluation

For a specified reflection, apparent lateral crystallite is calculated using the *Scherrer formula* as shown in equation (5) [40].

$$L_{hkl} = \frac{K\lambda}{\beta\cos(\theta)} \quad (4)$$

L_{hkl} is the average crystal length, K is the Scherrer parameter, λ is the radiation wavelength, β is the breadth at half-maximum intensity, θ is Bragg's angle of the related reflection.

Results and Discussion

In the manufacture of carbon fibers, the TOS is a mandatory step that is usually carried out in the air atmosphere. During the thermal stabilization, atmospheric

oxygen accelerates cyclization and oxidation reactions. In the present investigation, the effect of ammonium bromide impregnation of PAN fiber was investigated. Different structural changes take place in nitrile (C≡N) groups in the polymer structure and form a ladder-like structure for the chemical reactions in the TOS process.

Physical and Mechanical Properties Analysis

The TOS process of NH_4Br pretreated PAN fibers was performed by a multistep annealing method up to 250 °C temperature in the air for different stabilization times ranging from 5 to 75 min. Stabilized PAN fibers were exposed directly to a match flame to determine the burning behavior, and the test outcomes were classified as pass or fail. The color of the fibers gradually changes from white to golden-brown to blackish and black during thermal pretreatment with increasing stabilization time. Alteration of colors confirms the existence of a highly crosslinked aromatized structure of the stabilized PAN samples. The color of the fiber turned completely black of the 60 min multistep stabilized samples (Table 1).

The fiber thicknesses of the raw and stabilized PAN fibers measured for different stabilization times are presented in Table 1. With growing stabilization time, the fiber thickness of the stabilized samples was observed to decrease consistently. After a 5 min stabilization period, the fiber thickness dropped considerably, and the drop proceeded as the stabilization time increased. With a stabilization period of 75 min, the highest loss in fiber thickness was noticed, with around 36.56 %. The primary cause of decreased fiber thickness is thought to be the weight loss of the PAN fibers due to dehydration in the thermal stabilization stage.

With growing stabilization time, the linear density values reduced gradually (Table 1). After the 75 min stabilization time, a linear density fall of 44 % was noticed in the PAN samples and reached 51.07 tex from the value of 59.68 tex of the pristine PAN fiber. The exclusion of non-carbon elements, including hydrogen, nitrogen, H_2O, etc., is believed to be the cause of the significant reduction in linear density. The stabilization yield (%) reduced as the stabilization time increased, eventually dropping from 100 % to 89 % after 75 min multistep thermal stabilization.

Volume density values showed a continuous increase throughout the stabilization process. The volume density increased from 1.18 g/cm^3 of pristine PAN to 1.40 g/cm^3 of 75 min thermally stabilized samples because of the ongoing cyclization and oxidation reactions. The increase in volume density, comprised by the close packing of the molecular chains due to the cyclization of the nitrile bonds, is ascribed to creating a ladder-like pattern in the polymer [41].

The tensile strength of NH_4Br pretreated PAN samples revealed a significant dependence on the stabilization time. The 5 min multistep stabilized PAN lost 37.49 % tensile strength by reaching 158.61 MPa from 253.74 MPa of the pristine sample (Table 2). The value of tensile strength was continuously decreased with the increase of stabilization time and reached 81.14 MPa when it was stabilized for 75 min in the multistep approach. An intermolecular crosslinking process transforms nitrile (C≡N) bonds into nitrilo (C=N) during the TOS phase in the air environment. This transition results in a considerable loss of cohesive energy inside the polymer structure, which is the principal cause of tensile strength loss [42].

Strain to failure (%) of the pristine PAN sample was approximately 10.87 % (Table 2). However, thermal stabilization

Table 2. Mechanical properties of pristine and stabilized PAN fibers

Oxidation time (min)	Tensile strength (MPa)	Strain to failure (%)	Tensile modulus (GPa)
Pristine	253.74±30.06	10.87±3.57	14.18±2.42
5	158.61±23.50	6.81±1.03	9.25±1.51
15	126.20±25.35	4.29±1.11	10.89±1.38
30	107.80±15.39	2.89±0.95	11.34±1.13
45	94.79±16.88	1.83±0.55	11.78±1.16
60	84.81±21.42	1.35±0.45	11.81±1.81
75	81.14±19.80	1.30±0.26	12.99±2.10

*The values were expressed as means±standard deviations.

Table 1. Physical properties of pristine and stabilized PAN fibers

Oxidation time (min)	Color change	Flame test	Fiber thickness (μm)	Linear density (tex)	Volume density (g/cm^3)	Stabilization yield (%)
Pristine	White	Fail	21.99±0.15	59.68±0.11	1.18±0.04	100.00
5	Golden yellow	Fail	17.29±0.30	59.29±0.14	1.22±0.04	96.19
15	Golden brown	Fail	16.90±0.14	57.43±0.12	1.25±0.03	93.17
30	Dark brown	Fail	16.31±0.29	57.33±0.16	1.26±0.06	93.01
45	Blackish	Fail	16.30±0.26	55.18±0.13	1.35±0.03	89.52
60	Black	Pass	16.18±0.05	55.07±0.09	1.36±0.05	89.34
75	Black	Pass	13.95±0.10	51.07±0.20	1.40±0.04	89.00

*The values were expressed as means±standard deviations.

caused a great decrease of this measure of the PAN fibers. The decreasing tendency was noticed from 5 min multistep thermally stabilized samples with about 6.81 %, and reached around 1.30 % for 75 min multistep thermal stabilization. Table 2 represents the tensile modulus values of the pristine and NH_4Br incorporated-stabilized PAN samples. The tensile modulus of the pristine PAN was 14.18±2.42 GPa. A sharp decline of about 34.77 % was noticed in the 5 min multistep thermally stabilized samples. Afterward, this value gradually increased with the increase of stabilization duration and reached 12.99±2.10 GPa for 75 min multistep thermal stabilization.

X-ray Diffraction Analysis (XRD)

Analysis of XRD trace of untreated PAN fiber given in Figure 2 shows two ordered heights with d-distances of 0.538 and 0.309 nm, accredited to a hexagonal unit cell [26, 42,43]. The findings suggest that the ordered peaks (PE1 and PE3) could be ascribed to the (100) and (110) peaks of a hexagonal crystal structure with basal layer sizes of a=b=0.6 nm [42].

Table 3 shows that for stabilization periods between 5 and 75 min, d-spacing of the (100) reflection resulted in a 1.18 % lattice growth. In this instance, lattice enlargement of the (110) reflection was 0.68 % (Table 3). The X-ray diffraction traces also present an extra, less ordered, and wide peak (PE2) with a d-spacing of 0.346 nm (at approximately 25.5 ° 2θ) in Figure 2. Equatorial XRD curves of untreated and stabilized PAN fibers for different stabilization times are illustrated in Figure 3.

The lateral size of the (110) peak was dropped from 4.82 to 1.39 nm, according to the findings shown in Table 3. It also demonstrates the chain number in the hexagonal crystal structure estimated from the (110) planes based on the lateral crystal dimensions. The lateral crystal dimension for a 5 min stabilization period was estimated as five chains, while the

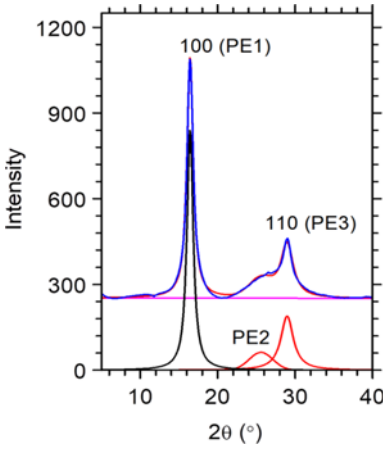

Figure 2. Curve-fitting of equatorial XRD curve of untreated PAN fibers.

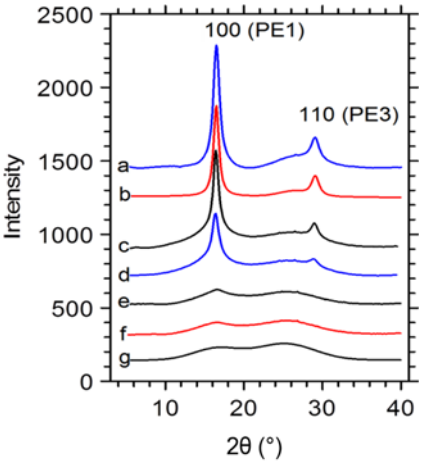

Figure 3. XRD curves of pristine (a), and stabilized PAN fibers for the stabilization times, (b) 5 min, (c) 15 min, (d) 30 min, (e) 45 min, (f) 60 min, and (g) 75 min.

untreated sample size conforms to 16 chains. The disordered peak (PE2) lateral dimensions varied between 2.54 and 0.7 nm when the stabilization times between 5 and 75 min. Because of continued stabilization reactions, the progressively occurring stabilization phase in the air led to a steady loss of apparent crystal structure and related decreased lateral crystallite size. The unoriented and disordered state can be attributed to this peak. The (002) reflection of the pre-graphitic structure (i.e., the aromatic/ladder) is ascribed to the d-space value of this peak [42].

The thermal stabilization process seems to have a great influence on crystalline structure in terms of crystal dimension and degree of crystallization. The curve fitting technique was utilized to determine precise peak characteristics in terms of peak position, peak height, and half breadth. A close investigation of Figure 4 reveals a steady loss of laterally ordered structure allotted to the hexagonal crystal phase by the progressing stabilization interactions [26,42,43]. The presence of the (100) reflection in the samples was observed for the stabilization times of 5, 15, and 30 min but weakened considerably in intensity for the samples stabilized for stabilization times of 45 min and higher. A comparable pattern was observed for the (110) reflection that stayed in a modest quantity throughout the stabilization process up to the 30 min multistep stabilization period but disappeared significantly during the stabilization times of 45 min and higher as a result of decrystallization reactions. Due to the use of equatorial XRD profiles, apparent X-ray crystallinity can be considered as an indicator of lateral order [42]. Equation (3) was used to calculate the apparent crystallinity values in this study. Curve fitting of the XRD traces led to practical assessment of apparent X-ray crystallinity and amorphous fraction (Figure 4).

The curve fitting technique was also used to obtain

Table 3. Analysis of XRD results of (110) reflection of the untreated and stabilized PAN samples

Stabilization period (min)	Peak position 2θ (deg)	Peak height	d-spacing (nm)	d-Spacing enlargement (%)	Corrected half-height width 2θ (deg)	Corrected crystallite size (nm)	No of chains
0	30.30	189.6	0.293	0.00	1.88	4.83	16
5	30.32	33.4	0.293	0.00	5.87	1.57	5
15	30.26	32.8	0.296	0.35	6.19	1.49	5
30	30.26	31.6	0.296	0.35	6.26	1.45	5
45	-	-	-	-	-	-	-
60	-	-	-	-	-	-	-
75	-	-	-	-	-	-	-

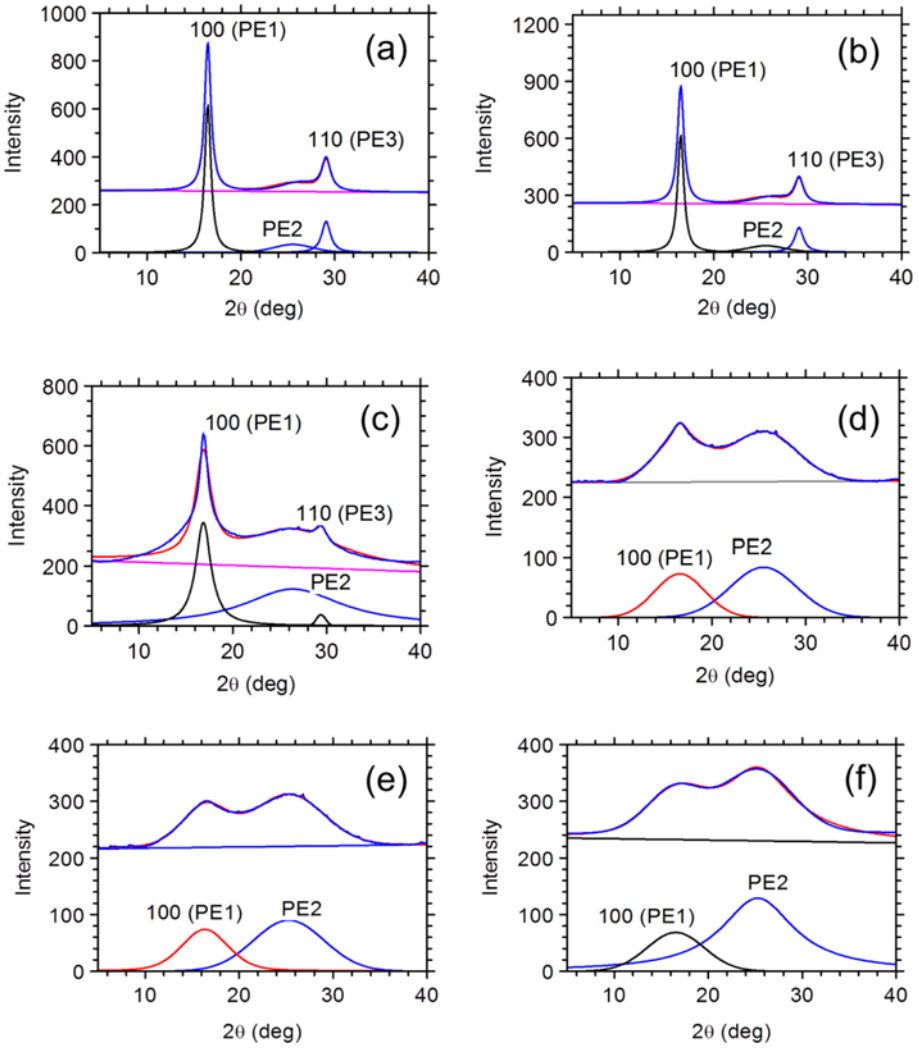

Figure 4. Curve fitting of equatorial XRD curves of stabilized PAN fibers for different stabilization times; (a) 5 min, (b) 15 min, (c) 30 min, (d) 45 min, (e) 60 min, and (f) 75 min.

accurate peak attributes, specifically peak heights above baseline, to assess X-ray stabilization indices employing equation (2). The X-ray stabilization index values in this study were seen to increase very rapidly as the stabilization time increased, which is considered to estimate the quantity of aromatic structure produced during stabilizing processes [42]. Figure 5 shows that apparent X-ray crystallinity values revealed a decreasing tendency from 19 to 5 %, while

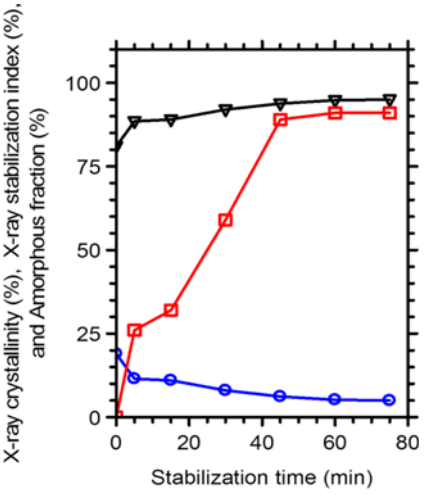

Figure 5. X-ray crystallinity, stabilization index, and amorphous fraction values with growing stabilization time. (○) X-ray crystallinity (%), (□) X-ray stabilization index (%), and (▽) Amorphous fraction (%).

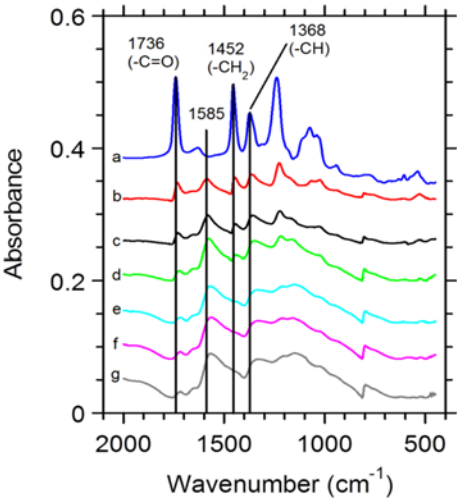

Figure 6. IR spectra of pristine (a), and stabilized PAN in the wavenumber range of 2000-450 cm^{-1} for stabilization times, (b) 5 min, (c) 15 min, (d) 30 min, (e) 45 min, (f) 60 min, and (g) 75 min.

amorphous fraction values grew over the stabilization periods. On the other hand, the amorphous fraction exposed the opposite tendency, growing from 81 to 95 % as the stabilization period increased.

For the determination of visible crystal dimensions, peak widths at half-height were employed and were corrected utilizing Stoke's deconvolution method. After the adjustment of instrumental broadening impacts relating to the ordered PE1 and PE3 peaks (100 and 110 respectively) utilizing Scherrer equation (4) of the pristine and stabilized PAN fibers, the lateral crystallite size was determined without regard for crystal perfection. The curve-fitting technique was used successfully to calculate exact peak specifications for the analysis of XRD profiles for determining lateral crystal dimensions attributed to the (100) and (110) ordered reflections. Table 3 and Table 4 represent adjusted half-height widths of ordered PE1 and PE3 reflections that were used to determine apparent crystallite sizes. The lateral size of the (100) reflection was decreased from 9.7 to 1.3 nm, according to the data shown in Table 4.

Infrared (IR) Spectroscopy Analysis

Infrared spectra of ammonium bromide impregnated and stabilized PAN samples showed significant structural changes compared to the original PAN spectrum, reflected by the intensity variations of the IR spectra with increasing stabilization time. Figure 6 represents a comparative analysis of infrared bands of original and stabilized PAN fibers for different treatment times in the 2000-450 cm^{-1} range. At 1736 cm^{-1}, the carbonyl (C=O) band of the aliphatic ketone group loses a major portion of its intensity after 5 min of residence time, then moves to a subordinate position as stabilization period increases, until it is apparent as a shoulder on the preceding conjugation absorption. This distinctive feature has been suggested as a possible indicator of the carbonyl bands being conjugated [44].

Because of the structural changes occurring during the

Table 4. Analysis of XRD results of (100) reflection of the untreated and stabilized PAN samples

Stabilization period (min)	Peak height	Peak position 2θ (deg)	d-spacing (nm)	d-spacing enlargement (%)	Corrected half-height width 2θ (deg)	Corrected crystallite size (nm)	Number of chains
0	842	16.48	0.538	0.0	0.92	9.7	18
5	614	16.48	0.538	0.0	0.93	9.6	18
15	539	16.42	0.539	0.19	0.95	9.4	17
30	308	16.42	0.539	0.19	0.97	9.2	17
45	21	16.40	0.540	0.37	1.53	5.8	11
60	11	16.27	0.544	1.11	1.97	4.5	8
75	7	16.27	0.544	1.11	7.08	1.3	2

TOS process, a new vibration at about 1585 cm^{-1} is observed in the IR spectra of NH_4Br impregnated-stabilized PAN sample. The IR vibration positioned at 1585 cm^{-1} is thought of as a sign of intramolecular reactions as well as the alteration of nitrile (C≡N) into nitrilo (C=N) band due to the incidence of aromatization processes [26]. In the published literature, different interpretations are made for the spectrum at 1585 cm^{-1}. In some investigations [44-46], it is assigned to a conjugated nitrilo (C=N) group arising from the formation of aromatization reactions. This spectrum is also ascribed to C=C and C=N vibrations by Clarke and Bailey [47]. Another assignment for the stabilized PAN sample is the composition of C=N, C=C, and N-H in-plane bending spectra [48]. The oxygen absorption processes are considered to be responsible for the existence of IR vibrations at 1583 and 1655 cm^{-1}. The attendance of oxygen-comprising groups, including conjugated ketone, aliphatic ketone, and hydroxyl groups in thermal stabilization processes indicates the presence of continuing oxygen uptake reactions. It is thought that oxidation reactions occur together with cyclization and dehydrogenation reactions. The C-C is transformed into a C=C entity that produces aromatic structures during the TOS phase, where oxygen is likely to keep a significant impact by aiding dehydrogenation processes.

The development of oxygen-containing functional groups including hydroxyl (-OH), carbonyl (-C=O), and carboxylic (-COOH) are thought to serve a secondary function of oxygen, which are compulsory for intermolecular crosslinking reactions in polymer structures, and also to have a role in the growth of structures with high thermal stability. During the carbonization reactions, the formation of intermolecular crosslinking reactions results in enhanced thermal stability and reductions in the formation of chain-breaking reactions [49]. The appearance of a new band at 1154 cm^{-1} suggests the development of a C-O group in carboxylic acids and α, β-unsaturated esters, which was based on oxygen inclusion reactions [50].

Due to the occurrence of dehydrogenation and the creation of C=C bonds, the $-CH_2$ and -C-O stretch at 1452 and 1233 cm^{-1}, correspondingly, turn out to be less prominent as treatment time increases (Figure 7). The IR-spectra between 1600 and 1300 cm^{-1} are categorized by a widening and intensification because of the generation of conjugated C-H (C=C-H) spectrum, which is ascribed to a new vibration creation at 806 cm^{-1} [51]. Just a few C=C groups are generated in the initial phases of the TOS and indicated as the instability of the band. The conjugated hydrocarbon structure is produced entirely as the thermal stabilization time increases, as shown by rising band intensity in the higher stabilization phases. In the wavenumber range from 3000 to 2800 cm^{-1}, two significant vibrations are positioned at 2920 and 2852 cm^{-1}, where the major methylene (CH_2) band is traced (Figure 7). The intensity fluctuation of the nitrile (C≡N) groups of PAN fiber is also noticeable as the

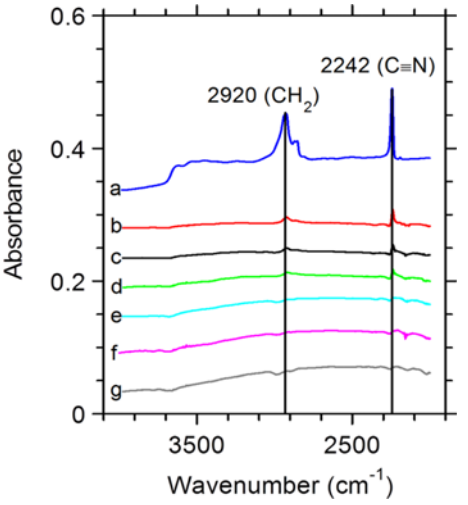

Figure 7. IR spectra of pristine (a), and stabilized PAN in the wavenumber range of 4000-2000 cm^{-1} for stabilization times, (b) 5 min, (c) 15 min, (d) 30 min, (e) 45 min, (f) 60 min, and (g) 75 min.

stabilization time increases. The nitrile (C≡N) band is centered at around 2242 cm^{-1}. Within 5 min of multistep TOS process, the methylene (CH_2) bands lose most of their intensity, indicating that hydrogen atoms are eliminated, owing to the occurrence of dehydrogenation in the polymer chain along with the development of a crosslinked pattern. In the TOS procedure, oxygen is partially integrated with the PAN fibers by the dehydrogenation processes. At 2242 cm^{-1}, the nitrile band shows a rapid decrease of intensity; meanwhile, at approximately 2120 cm^{-1}, a new band corresponding to thiocyanate (S=C=N) stretching emerges [50].

Thermally stabilized PAN samples demonstrate a greater intensity loss of nitrile groups in the oxygen-rich air at increased temperatures [47]. The IR bands between the 3700 and 2300 cm^{-1} region, characterized by a methylene vibration (CH_2), contain a major band at 2920 cm^{-1} that is partly retained but considerably reduced in intensity even after 75 min multistep heating. The loss of hydrogen atoms causes dehydrogenation processes in the main polymer chains, as directed by the steady loss of intensity of the methylene groups at 2920 cm^{-1}.

Figure 8 represents the intensity variations of nitrile (C≡N) groups of polyacrylonitrile polymer for different residence times. By the growth of the thermal stabilization stages, continuous peak height decrease of the nitrile group directs to the incidence of the aromatization reactions. With increasing residence time, methylene (CH_2) intensity in-plane bending and aliphatic methylene (CH_2) bands at 1452 and 2920 cm^{-1} weakens, followed by an increased conjugation =C-H spectrum at 806 cm^{-1}, indicating the creation of a conjugated polymer structure. The specific peak heights in absorbance mode utilized to assess the dehydrogenation

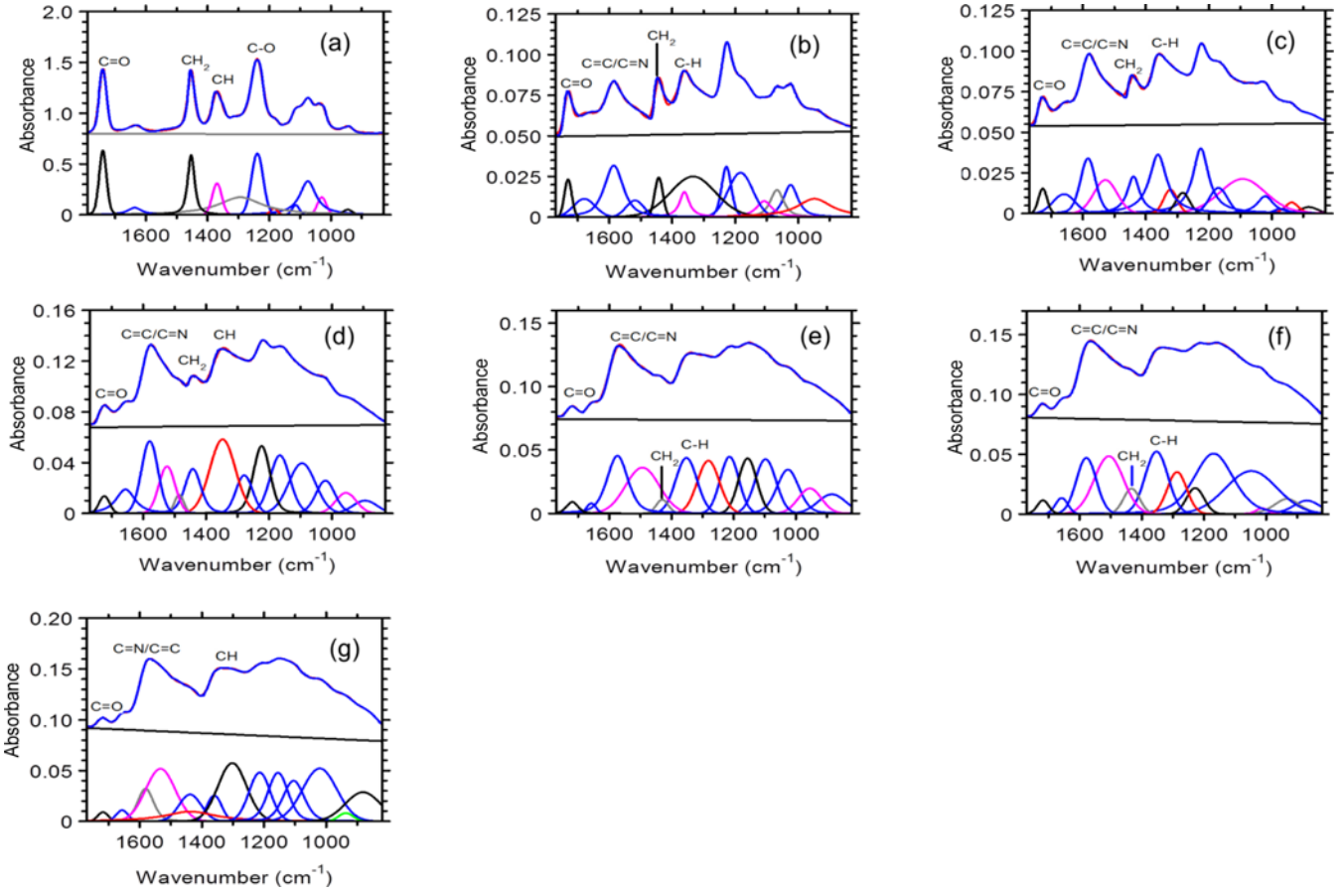

Figure 8. Curve fitting of IR spectra in the 1850-850 cm^{-1} region of pristine (a), and stabilized PAN for different stabilization times. (b) 5 min, (c) 15 min, (d) 30 min, (e) 45 min, (f) 60 min, and (g) 75 min.

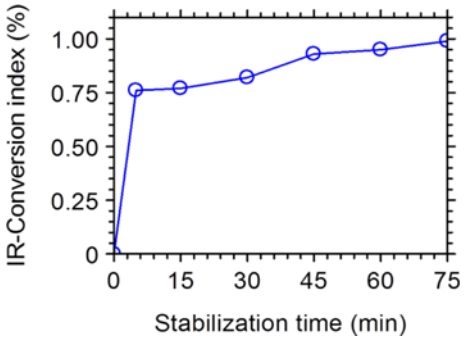

Figure 9. IR-conversion index of pristine and stabilized PAN fiber for different stabilization times.

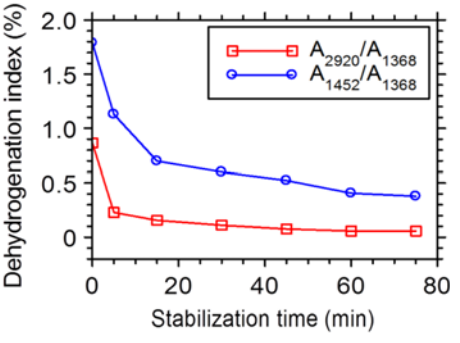

Figure 10. Dehydrogenation index variations of pristine and stabilized PAN fibers.

index (A_{1432}/A_{1366}) were obtained using the infrared curve fitting technique for the bands at the 1850-850 cm^{-1} region.

By utilizing the nitrile group at 2242 cm^{-1} and conjugated structure band at 1583 cm^{-1}, the IR-conversion index was estimated using equation (1) to assess the conversion of structures into a highly crosslinked and cyclized structure. NH_4Br impregnated PAN fibers exhibit quick transformation of untreated PAN to a highly aromatized structure, as shown in Figure 9. The IR-conversion index is usually utilized to assess the growth of ladder pattern formation in a polymer that is quicker in the early stages but slows as the stabilization period increases. The IR-conversion index value grows quickly within the first 5 min of the multistep TOS process, reaching 75 % and then progressively slowed

and reached 98 % after 75 min of multistep stabilization. The IR spectroscopy study revealed that the change of polyacrylonitrile structure into crosslinked ladder-like structure started in 5 min of multistep TOS process of the PAN fiber.

The dehydrogenation indices indicate the continual hydrogen atom loss caused by dehydrogenation processes that were measured employing the absorbance ratios A_{2920}/A_{1368} and A_{1452}/A_{1368} as illustrated in Figure 10. The results suggest accelerated dehydrogenation processes. As a result, the hydrogen content declines as the dehydrogenation index values drop. So, a strong correlation is thought to be present in the dehydrogenation index and the loss of hydrogen atoms from the polymer structure. Because of the enhanced dehydrogenation reactions, NH_4Br incorporation with PAN fibers accelerates the conversion of the C-C into a C=C bond.

Thermal Analysis (TGA)

In the current investigation, TGA characterization was utilized for the structural analysis of the ammonium bromide impregnated PAN fibers. Quantitative analyses of TGA thermograms are commonly performed to acquire carbon yield values that are regarded as an important evaluation method for stabilized PAN fibers. During the carbonization phase, significant weight losses of these stabilized fibers occur through elimination reactions resulting in various pyrolysis by-products. Typically, components excluding carbon are expelled in the course of carbonization reactions from the untreated PAN fibers in the temperature interval of 200-600 °C and higher. Transformation of untreated PAN fibers from a chain to a cyclic structure leads to a heat-resistant form and the removal of water vapor, CO_2, CO, HCN, N_2, O_2, H_2, etc., atoms during the stabilization and carbonization stages [44,52].

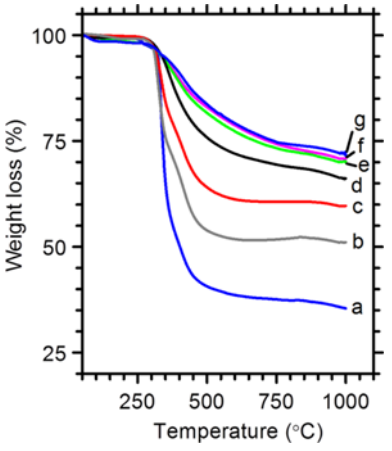

Figure 11. TGA thermograms of pristine (a) and stabilized PAN fibers for stabilization times, (b) 5 min, (c) 15 min, (d) 30 min, (e) 45 min, (f) 60 min, and (g) 75 min.

The TGA thermograms of pristine and NH_4Br integrated PAN samples are illustrated in Figure 11, which direct the two-step degradation mechanism occurring in the PAN fibers. The thermal stability of the samples remains unchanged from 50 to 200 °C without any significant weight loss. A slow rate of degradation was noticed at the temperature range from 200 to 300 °C. However, in the temperature range between 300 and 450 °C, a rapid mass loss of the PAN samples was observed. TGA thermograms of stabilized PAN samples exhibit growing carbon yield and thermal stability because of the impact of the enhanced intramolecular and intermolecular crosslinking and aromatization reactions caused by the addition of NH_4Br in the PAN fiber structure.

TGA thermograms presented in Figure 11 indicate the increase in carbon yield with the growth of stabilization time, which directs a decrease in mass loss caused by the progressing aromatization process. The weight loss steadily decreases between 50 and 450 °C as the stabilization time gets longer. Stabilized PAN samples between 300 and 450 °C undergo severe thermal degradation in 5 min stabilization, with mass loss of 53.4 % at 500 °C and 50.5 % at 1000 °C. Stabilized PAN Samples lose 17 % weight at 500 °C and 28 % at 1000 °C after 75 min of stabilization. Analysis of the TGA thermograms shows that due to the formation of oxidation-based crosslinking and aromatization reactions, the PAN fibers gain superior thermal stability.

For 500 °C and 1000 °C temperatures, carbon yields of pristine and NH_4Br integrated-stabilized PAN fiber are presented in Figure 12. With the progress of stabilization periods between 5 and 75 min, continuous growth in carbon yield was noticed. At 500 and 1000 °C, the carbon yield percentage for the 5 min multistep stabilized PAN fibers was 54 and 51 %, respectively. The highest carbon yield value in the investigation was 83 % at 500 °C, and 72 % at 1000 °C for the 75 min stabilized PAN fiber (Figure 12).

Figure 13 depicts the dTGA pattern of the TGA thermograms. Between the 300 to 400 °C temperature range, exothermic peaks of the dTGA curves are noticed for the

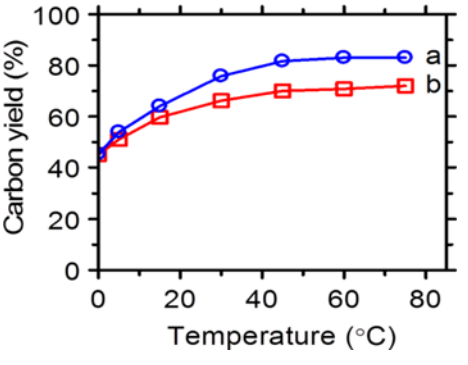

Figure 12. Carbon yield (%) of pristine and stabilized PAN fibers for different stabilization times at temperatures of 500 °C (a), and 1000 °C (b).

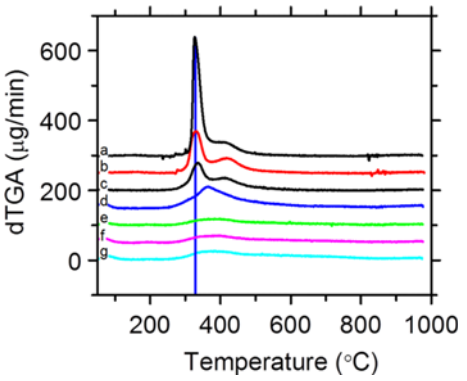

Figure 13. dTGA thermograms of pristine (a), and stabilized PAN fibers for stabilization times, (b) 5 min, (c) 15 min, (d) 30 min, (e) 45 min, (f) 60 min, and (g) 75 min.

untreated PAN fiber. The dTGA thermograms for stabilized PAN fibers shift to 410 °C after the TOS processes, and a new peak emerges at 330-380 °C. The exothermic peak located at 330 °C is prominent in intensity in comparison with the peak at 400 °C. These peaks are assigned to the aromatization and cyclization processes of the PAN fibers with the discharge of different by-products containing acetonitrile, acrylonitrile, benzonitrile, crotonitrile, propane, dicyanobutene, HCN, and dicyanobenzene [53]. The peak observed at 100 °C is assigned to the presence of water. From the results obtained, it can be seen that aromatization reactions occur because of the formation of (C=N) bonds resulting in the creation of ring structures [54]. The cyclization reaction of nitrile bonds occurring in the TOS process causes entirely new molecular structures. The broadening of the exothermic peak observed in Figure 13 is thought to be related to the formation of cyclic structures occurring in the course of thermal stabilization. The steady reduction of exothermic peak heights due to aromatization reactions with growing stabilization periods as mentioned in Table 5. When the exothermic peaks disappear completely, it signifies that the intramolecular aromatization processes are completed at higher stabilization temperatures.

Table 5. dTGA results of the pristine and stabilized PAN samples

Stabilization time (min)	1st Peak temperature (°C)	1st Peak temperature height	2nd Peak temperature (°C)	2nd Peak temperature-height
0	330	336	420	40
5	330	120	412	40
15	332	78	408	34
30	360	60	408	20
45	380	25	-	-
60	380	18	-	-
75	380	18	-	-

Conclusion

Ammonium bromide impregnation was carried out for PAN fibers prior to thermal stabilization experiments. The results suggested faster thermal stabilization reactions resulting in the rapid formation of aromatized structures in the NH_4Br integrated-stabilized PAN fibers necessary to tolerate higher carbonization temperatures and meanwhile reducing the stabilization time before the carbonization step. The physical, structural and thermal properties of stabilized PAN fibers were evaluated using IR spectroscopy, equatorial XRD, TGA, tensile testing, volume density, linear density, and fiber thickness measurements. For stabilization periods of 5 and 75 min, volume density values ranged between 1.22 and 1.42 g/cm^3. The quantitative analysis of equatorial XRD profiles was used to follow and describe structural changes to a completely amorphous state. A curve-fitting procedure was used to calculate average crystallite size using Stoke's deconvolution method. Quantitative analysis of equatorial XRD traces indicated the loss of lateral order as shown by the reduced crystallite size and the intensity of the (100) reflection assigned to a hexagonal unit cell. The formation of dehydrogenation and aromatization processes, aided by the take up of oxygen in the TOS process, appears to be a direct result of the conversion of molecular structure from a highly ordered to an entirely disordered amorphous state. The attendance of oxygen in the molecular structure of the stabilized PAN multifilament was confirmed by the presence of hydroxyl (OH), carboxyl (COOH), carbonyl (C=O) functional groups. IR spectroscopy findings specified a quicker and constant dehydrogenation and cyclization process as the stabilization duration increased, as demonstrated by the quick intensity decrease of the methylene band at 2920 cm^{-1} and the nitrile band at 2242 cm^{-1}. TGA study revealed the integration of NH_4Br improves carbon yield and thermal stability significantly over untreated PAN specimens. As a whole, the experimental results suggest that NH_4Br impregnation with PAN fiber may keep a significant contribution in carbon fiber manufacturing by reducing overall processing expense and time once the other operating conditions are controlled accurately.

Acknowledgements

This study was supported by the YÖK 100/2000 Micro and Nano Technology Materials PhD scholarship of the Higher Education Council of Turkey to Tuba DEMIREL.

Conflicts of Interest

There is no conflict of interest among the authors.

References

1. O. Zabihi, M. Ahmadi, Q. Li, S. Shafei, M. G. Huson, and M. Naebe, *Compos. Sci. Technol.*, **148**, 49 (2017).
2. D. D. Edie, *Carbon*, **36**, 345 (1998).
3. W. X. Zhang and M. S. Li, *J. Mater. Sci. Technol.*, **21**, 581 (2005).
4. X. Huang, *Materials*, **2**, 2369 (2009).
5. D. Sawai, Y. Fujii, and T. Kanamoto, *Polymer*, **47**, 4445 (2006).
6. C. Hou, R. Qu, J. Liu, L. Ying, and C. Wang, *J. Appl. Polym. Sci.*, **100**, 3372 (2006).
7. T.-H. Ko, S.-C. Liau, and M.-F. Lin, *J. Mater. Sci.*, **27**, 6071 (1992).
8. N. An, Q. Xu, L. H. Xu, and S. Z. Wu, *Adv. Mater. Res*., **11**, 383 (2006).
9. L. Jie and Z. Wangxi, *J. Appl. Polym. Sci.*, **97**, 2047 (2005).
10. B. A. Newcomb, *Compos. Part A Appl. Sci. Manuf.*, **91**, 262 (2016).
11. K. Xia, Q. Ouyang, Y. Chen, X. Wang, X. Qian, and L. Wang, *ACS Sustain. Chem. Eng.*, **4**, 159 (2016).
12. E. A. Morris, M. C. Weisenberger, M. G. Abdallah, F. Vautard, H. Grappe, S. Ozcan, F. L. Paulauskas, C. Eberle, D. Jackson, and S. J. Mecham, *Carbon*, **101**, 245 (2016).
13. P. J. Sanchez-Soto, M. A. Aviles, J. C. D. Rıo, J. M. Gines, J. Pascual, and J. L. Perez-Rodrıguez, *J. Anal. Appl. Pyrol*., **58**, 155 (2001).
14. J. Liu, S. Xiao, Z. Shen, L. Xu, L. Zhang, and J. Peng, *Polym. Degrad. Stab.*, **150**, 86 (2018).
15. N. Tajaddod, H. Li, and M. L. Minus, *Polymer*, **137**, 346 (2018).
16. H. Mirbaha, S. Arbab, A. Zeinolebadi, and P. Nourpanah, *Smart Mater. Struct.*, **22**, 45019 (2013).
17. N. Yusof and A. F. Ismail, *J. Anal. Appl. Pyrol*., **93**, 1 (2012).
18. P. Rangarajan, J. Yang, V. Bhanu, D. Godshall, J. McGrath, G. Wilkes, and D. Baird, *J. Appl. Polym. Sci.*, **85**, 69 (2002).
19. Z. Wangxi, L. Jie, and W. Gang, *Carbon*, **41**, 2805 (2003).
20. D. He, C. Wang, Y. Bai, and B. Zhu, *J. Mater. Sci. Technol.*, **21**, 376 (2005).
21. E. Frank, F. Hermanutz, and M. R. Buchmeiser, *Macromol. Mater. Eng.*, **297**, 493 (2012).
22. N. U. Nguyen-Thai and S. C. Hong, *Macromolecules*, **46**, 5882 (2013).
23. J. Hao, Y. Liu, and C. Lu, *Polym. Degrad. Stab.*, **147**, 89 (2018).
24. G. Golkarnarenji, M. Naebe, K. Badii, A. S. Milani, R. N. Jazar, and H. Khayyam, *Comput. Chem. Eng.*, **109**, 276 (2018).
25. G. Golkarnarenji, M. Naebe, K. Badii, A. S. Milani, R. N. Jazar, and H. Khayyam, *Materials*, **11**, 385 (2018).
26. I. Karacan and G. Erdoğan, *Polym. Eng. Sci.*, **52**, 937 (2012).
27. I. Karacan and T. Soy, *J. Appl. Polym. Sci.*, **128**, 1239 (2013).
28. I. Karacan and G. Baysal, *Fiber. Polym.*, **13**, 864 (2012).
29. M. M. Rahman, T. Demirel, K. Ş. Tunçel, and I. Karacan, *J. Mater. Sci.*, **56**, 14844 (2021).
30. J. Troitzsch, "International Plastics Flammability Handbook", Munich, Hanser Gardner Publications, 1990.
31. J. H. Troitzsch, *Chim. Oggi/Chemistry Today*, **16**, 18 (1998).
32. S. Mostashari, H. Moafi, and S. Mostashari, *J. Therm. Anal. Calorim.*, **96**, 535 (2009).
33. I. Karacan and G. Erdoğan, *J. Inorg. Organomet. Polym. Mater.*, **22**, 1016 (2012).
34. D. P. Bahl, R. B. Mathur, and T. L. Dhami, *Mater. Sci. Eng.*, **73**, 105 (1985).
35. W. Sweeny, "Cyclization of Acrylic Fiber", US4603041 (1986).
36. S. Sikkanthar, S. Karthikeyan, S. Selvasekarapandian, D. V. Pandi, S. Nithya, and C. Sanjeeviraja, *J. Solid State Electrochem.*, **19**, 987 (2015).
37. Y. Zhu, M. A. Wilding, and S. K. Mukhopadhyay, *J. Mater. Sci.*, **31**, 3831 (1996).
38. M.-J. Yu, Y.-J. Bai, C.-G. Wang, Y. Xu, and P.-Z. Guo, *Mater. Lett.*, **61**, 2292 (2007).
39. A. M. Hindeleh and D. J. Johnson, *Polymer*, **19**, 27 (1978).
40. A. R. Stokes, *Proc. Phys. Soc.*, **61**, 382 (1948).
41. P. Bajaj and A. K. Roopanwal, *J. Macromol. Sci. Part C Polym. Rev.*, **37**, 97 (1997).
42. I. Karacan and G. Erdoğan, *Fiber. Polym.*, **13**, 855 (2012).
43. I. Karacan and G. Erdŏgan, *Polym. Eng. Sci.*, **52**, 467 (2012).
44. N. Grassie and R. McGuchan, *Eur. Polym. J.*, **8**, 257 (1972).
45. J. J. Rafalko, *J. Polym. Sci. Polym. Phys. Ed.*, **22**, 1211 (1984).
46. N. Grassie and R. McGuchan, *Eur. Polym. J.*, **7**, 1091 (1971).
47. A. J. Clarke and J. E. Bailey, *Nature*, **243**, 146 (1973).
48. I. Shimada, T. Takahagi, M. Fukuhara, K. Morita, and A. Ishitani, *J. Polym. Sci. Part A Polym. Chem.*, **24**, 1989 (1986).
49. M. S. A. Rahaman, A. F. Ismail, and A. Mustafa, *Polym. Degrad. Stab.*, **92**, 1421 (2007).
50. E. V. Loginova, I. V. Mikheev, D. S. Volkov, and M. A. Proskurnin, *Anal. Methods*, **8**, 371 (2016).
51. T. Chung, Y. Schlesinger, S. Etemad, A. G. Macdiarmid, and A. J. Heeger, *J. Polym. Sci. Polym. Phys. Ed.*, **22**, 1239 (1984).
52. A. G. Dumanlı and A. H. Windle, *J. Mater. Sci.*, **47**, 4236 (2012).
53. G. Leal and J.-I. Peñaloza, *CT&F-Ciencia, Tecnol. y Futur.*, **2**, 41 (2002).
54. S. Kim, Y. S. Chung, H.-S. Choi, F.-L. Jin, and S.-J. Park, *Bull. Korean Chem. Soc.*, **34**, 3733 (2013).